SMiRT-12 / K. Kussmaul (Editor)

FG15/2

CREEP-FATIGUE CRACK INITIATION AND GROWTH ON THICK CIRCUMFERENTIALLY NOTCHED 316L TUBES UNDER CYCLIC THERMAL SHOCKS AND UNIFORM TENSION

C. Poette and S. Albaladejo

CEA, DER/SERA - CEN Cadarache, F-13108 Saint Paul Lez Durance Cedex, France

SUMMARY

A validated methodology for the assessment of flaws in the creep-fatigue regime is needed for safety studies in fast reactor applications.
A usual appproach, but often too conservative, leads to consider all the types of situations as load controlled ones for the analysis.
The TERFIS test program performed at CEA Cadarache has the objective to give quantitative estimations of initiation times and subsequent crack growth of flaws in representative creep-fatigue conditions of the LMFBR structures (low primary stresses, high secondary stresses).
The structures tested are thick 316L tubes with inner radius to thickness ratio Ri/t of 1.5 and complete circumferential inner wall electro-eroded notches submitted to uniform tension and cyclic thermal shocks giving rise to radial temperature gradients. The cycles are separated by dwells of 2 hours at 600°C.
After a brief description of the test device, the present work gives some first results and interpretation using a proposed methodology involving elasto-plastic finite elements calculations.

1 INTRODUCTION

In the recent years, for the purpose of Fast Breeder Reactor applications, the need appeared for improved methods of flaw evaluation at temperatures where significant creep is involved.
More generally, these problems are discussed at the french level within a RCC-MR comittee working group (see also paper (1) of the present SMIRT 12) and at the European level (AGT 9B til March 93).
The aim is to identify reliable methods for application to realistic situations with all their possible complexity.
It is generally easier, but often too conservative, to consider all the loading situations as load controlled ones for the analysis of defects.
The TERFIS test program has the objective to give quantitative estimations of initiation times and creep-fatigue crack growth of flaws submitted to representative loadings typical of FBR structures (low primary stresses, large secondary stresses).

2 TEST DEVICE DESCRIPTION

Fig. 1 shows a general scheme of the test device. Thick 316L (N) tubes with an internal complete circumferential surface electro-eroded notch are submitted to uniform constant axial tension and cyclic thermal shocks.
Three tubes are cycled simultaneously, a fourth beeing used for thermal data logging.
The geometrical characteristics and loading conditions are the following for the first serie of tests :

- internal radius Ri = 18 mm
- thickness t = 12 mm
- crack depths a = 4, a = 5.5 and a = 7 mm
- specimen length L = 120 mm

The primary load is applied by means of a pneumatic jack. The corresponding axial nominal stress was Pm = 29 MPa.

The secondary loading is made of cyclic thermal shocks obtained by injecting cold sodium at 200°C outside the tube after prior temperature dwell at 600°C with static 600°C hot sodium inside the tube. Intercycle dwell times were fixed at 2 h at 600°C.

3 RESULTS OF THE FIRST SERIE OF TESTS

3.1 Mechanical results

After cycling, each sample was examined by metallographic microscopy. (longitudinal planes at 90° intervals were cut).

The results obtained are summarized in the following table :

Sample number	a_o/t (mm/mm)	a_f/t (mm/mm)	Δa (mm)	Number of cycles	Total dwell at 600°C (h)
4	7/12	12/12 (*)	5	232	464
3	5.5/12	10/12	4.5	282	564
2	4/12	6.5/12	2.5	295	590

(*) Test ended with guillotine failure of the sample.

Notations :

a_o initial notch depth

a_f final crack depth

$\Delta a = a_f - a_o$

The propagation observed was relatively axisymmetric and mainly of the intergranular type, as expected for these tests performed in the creep regime.

(See figures 2 and 3 illustrating crack propagation from the initial notches of samples number 2 and 3 respectively).

3.2 Thermal results

Figure 4 shows the time-temperature through the wall distribution during a thermal shock.

From a simple one-dimensional thermal model, the maximum equivalent linear temperature gradient was identified. Its value was ΔT_1 = 300°C.

4 MECHANICAL ANALYSIS

4.1 Mechanical mecanisms description

Figure 5 illustrates the stress state during thermal shock and subsequent residual stress state during dwell time (due to cyclic plastification).

Figure 6 illustrates the difference expected between an elastic (points 1 and 2) and an elasto-plastic (points 3 and 4) analysis of the problem in terms of stress-strain behaviour near the initial notch tip. Tensile stresses at point 4, particularly, are composed of residual stresses due to thermal shock (main loading) added to the primary tensile stress due to the axial force. These tensile stresses, acting during each dwell time at a uniforme temperature of 600°C, are responsible for creep damage at notch tip.

4.2 Elastoplastic analysis

Evaluations of initiation times based on σd approach (1) showed that the initiation occured very soon (less than 10 cycles) and the analysis presented here is focussed on propagation.

It is possible to estimate the propagation per cycle separating fatigue and creep propagation using :

$$da/dN = (da/dN)_{fatigue} + \int_o^{tm} \mathring{a}\,(C^*)\,dt$$

where : tm is the dwell time per cycle.
$\mathring{a}(C^*)$ is the creep crack growth rate versus the creep energy rate line integral parameter C* (2).

C* is calculated using a simplified method :

$C^* = l_{ref}\,\sigma_{ref}\,\dot{\epsilon}(\sigma_{ref})$

The l_{ref} term, or reference length was choosen as l_{ref} = t-a from R. Picques work on 316L (N) (3) rather than the general usual, but very conservative term $l_{ref} = K_I^2/\sigma_{ref}^2$ from (2).

For the particular type of loading considered here, the σ_{ref} term can be understood as the maximum stress in the ligament excluding peak stresses.

This reference stress can be separated in two terms, a primary part independent of time, and a secondary part allowing creep relaxation.

$\sigma_{ref}(t) = \sigma_{ref\,P} + \sigma_{ref\,S}(t)$

The stress relaxation $\sigma_{ref\,S}$ (t) is calculated following the french RCC-MR code RB 3200 and particularly RB-3262-12 (4) using power creep laws at 600°C from Appendix A3-1S for 316L (N).

For the initial σ_{ref} estimation, we have performed direct finite elements cyclic elastoplastic calculations on the initial notch geometry using CEA CASTEM (5). Figure 7 shows a detailed view of the mesh used around the notch (the notch root radius is 0.1 mm). For plasticity we used a non linear kinematic hardening 5 parameters Chaboche type model. The parameters were identified on the cyclic stress strain curve of the material drawn from Appendix A3-1S (4) at 600°C extrapolated til $\Delta\epsilon p$ = 5 %. Other material properties such as Young's modulus and thermal expansion coefficient were also drawn from A3-1S at 600°C.

Figure 8 shows the Von Mises and meridional residual stress distribution across the ligament after 2 cycles (sufficient for stress stabilization) at the uniform temperature 600°C for a_o = 4 mm, case choosen for the application.

The results allowed the identification of :

$\sigma_{ref\,P}$ = 40 MPa and $\sigma_{ref\,S}$ = 218 MPa

For crack growth rate we used an envelope AEA law for 316L (N) : da/dt = $2.17.10^{-2}$ $(C^*)^{0.81}$
(m/h) (MPa.m/h)

The results obtained are gathered in the following table :

Case	σ_{ref} (t=0) MPa	σ_{ref} (t=2 h) MPa	Δa (μ) enveloppe law	Δa (μ) mean law (*)	Mean experi-mental Δa (μ)
1) Pure creep (Cr=∞)	258	258	311	43	
2) Creep-relaxation (Cr=3)	258	227	203	28.4	7.1 (for a_o=4mm)
3) Creep pure relaxation (Cr=1)	258	201	132	18.5	

(*) The mean law is the enveloppe law divided by 7.14
The different cases 1, 2 and 3 are related to different degrees of severity supposed for the secondary loading (coefficient Cr of RCC-MR)

The contribution per cycle due to fatigue using a classical Paris enveloppe equation for 316L(N) at 600°C is $\Delta a = 2.5\ \mu$ (ΔK = 52.5 MPA $\sqrt{m}$, R = Kmin/Kmax = -13.1).

We can see that, in every cases, the calculated propagation per cycle using separated fatigue and creep contributions gives conservative results when compared to the experimental propagation.

It is clear that this doesn't mean that no creep fatigue interaction exist, but simply that the described route could be used for conservative engineering applications.

5 CONCLUSION

The TERFIS test program devoted to creep fatigue flaw evaluation and the results of the first serie of tests focussed on propagation were presented. Other series of tests devoted to initiation, to cracks in weldments, or to semi-elliptical cracks for Leak Before Break support are currently performed within this program.

The interpretation of the first results using a methodology separating creep and fatigue propagation and involving elasto-plastic finite elements calculations is encouraging but need further confirmation. The identification of the test material properties on CT specimens which is part of the program will allow a full validation of the method.

Acknow ledgments : this work was sponsored by EDF.

REFERENCES

[1] B. DRUBAY, D. MOULIN, C. FAIDY, C. POETTE, S. BHANDARI
Defect Assessment procedure : a french approach for fast breeder reactors SMIRT 12 - Division G - Stuttgart, 1993.

[2] CEGB Assessment procedure for defects in plant operating in the creep range. R.A. Ainsworth and al. Fatigue of Engineering Materials and Structures
Vol. 10, n° 2, pp. 115-127, 1987.

[3] Mécanique et mécanisme de l'amorçage et de la propagation des fissures en viscoplasticité dans un acier inoxydable austénitique. Thesis presented by R. Picques (February 1989). ENSMP, Paris

[4] AFCEN (1985) Règles de conception et de construction des matériels mécaniques des îlots nucléaires RNR. RCC-MR AFCEN Janvier 1985.

[5] CASTEM (CEA SEMT) A system of finite elements computer programs paper 40, Proc. Conf. Struct. Anal. Design Construction of Nuclear Power Plants.
Porto Alegre, Brazil (1978).

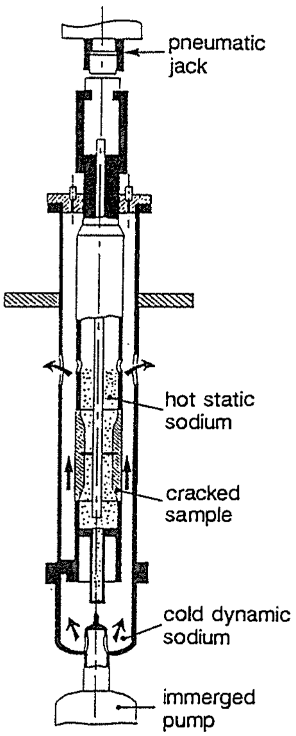

Figure 1 : GENERAL VIEW OF TERFIS TEST DEVICE

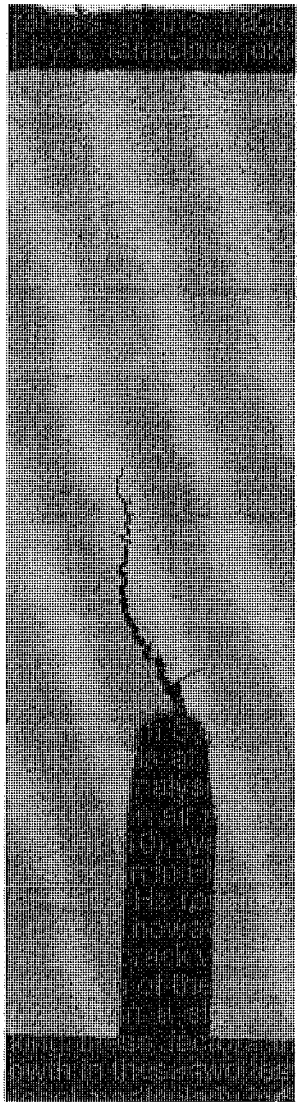
Figure 2: INTERGRANULAR PROPAGATION IN SAMPLE 2

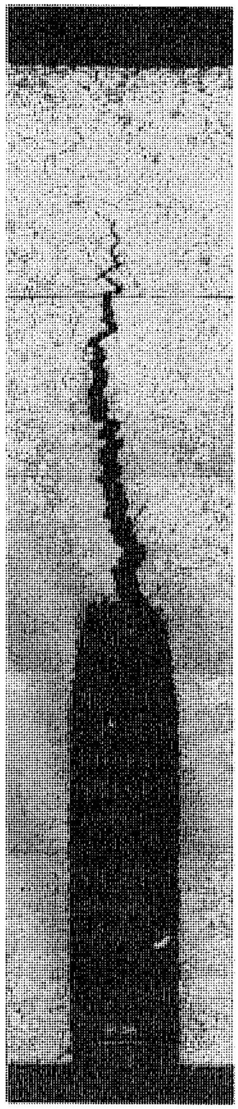
Figure 3: INTERGRANULAR PROPAGATION IN SAMPLE 3

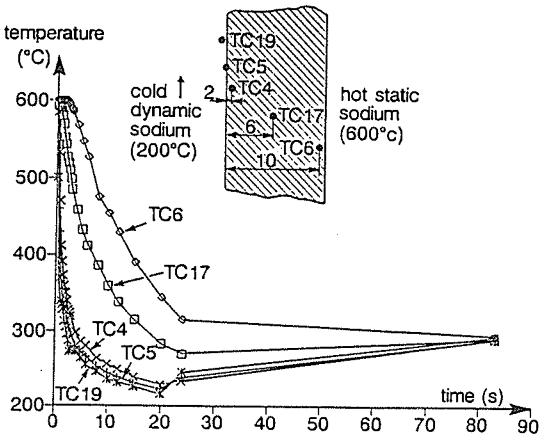

Figure 4 : TIME-TEMPERATURE THROUGH THE WALL DISTRIBUTION DURING THERMAL SHOCK

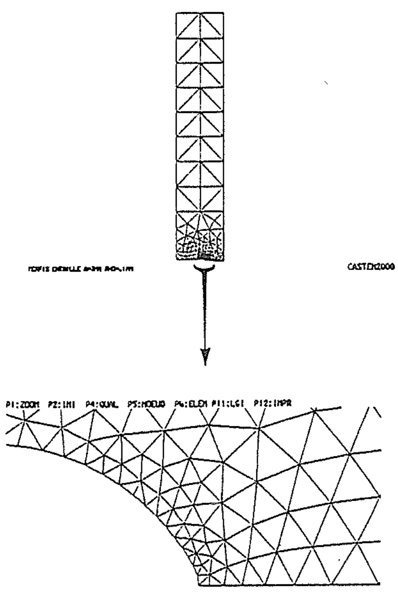

Figure 7 : TYPE OF F.E. MESH USED FOR ELASTO-PLASTIC NOTCH CALCULATION

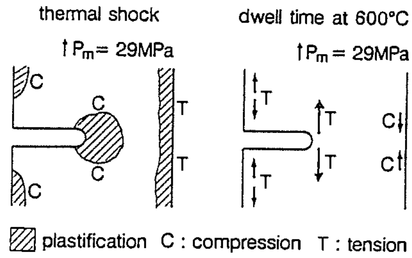

Figure 5 : PRINCIPLE OF THE LOADING

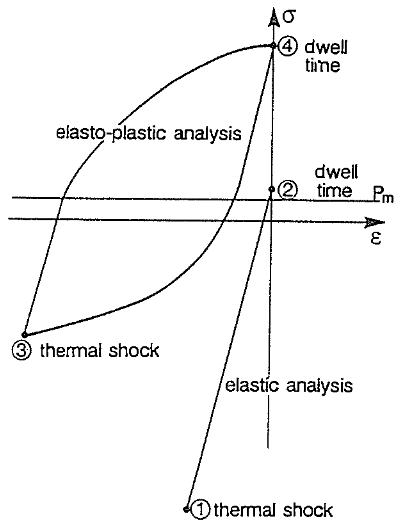

Figure 6 : QUALITATIVE STRESS-STRAIN RELATIONS NEAR NOTCH TIP

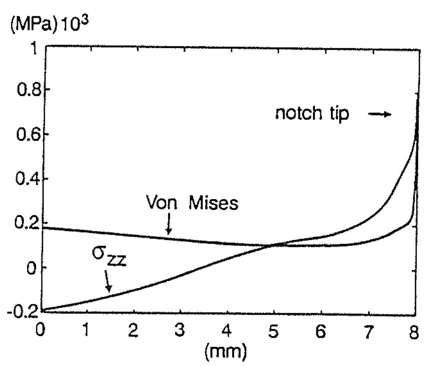

Figure 8 : VON MISES AND MERIDIONAL RESIDUAL STRESS DISTRIBUTION AFTER THE SECOND CYCLE